

JUN 26 1989

POSITIVE POLARITY VOLTAGE ADDER MITL EXPERIMENTS ON HELIA*

J. P. Corley, C. E. Heath, D. L. Johnson,
 S. E. Rosenthal, J. W. Poukey, J. J. Ramirez
 Sandia National Laboratories
 Albuquerque, New Mexico 87185

SAND--89-0080C
 DE89 014705

I. D. Smith, P. W. Spence, J. J. Fockler
 Pulse Sciences, Inc.
 San Leandro, California 94577

Abstract

HELIA is a four stage, 4-MV, 250-kA, 30-ns accelerator used to study the design concepts for Hermes III. The accelerator consists of eight pulse forming lines (PFLs) that deliver 1-MV, 125-kA pulses to four linear induction cavities. The cavities are in series, and the voltage addition is accomplished in a coaxial self magnetically insulated transmission line (MITL).

A positive polarity experiment has been performed on Hermes III that shows efficient current transport through the system. HELIA has been reconfigured for positive polarity operation, and initial experimental results show operation consistent with Hermes III results. These experiments are aimed at obtaining a more complete understanding of the system performance in positive polarity and to investigate the interactions of the cavities, adder MITL, and extensions in this configuration. Initial results and details of these tests are presented in this paper.

Introduction

Figure 1 is a photograph of HELIA. HELIA is a four stage, 4-MV, 250-kA, 30-ns FWHM accelerator¹ that was used as a proof-of-principle experiment for the 22-MV, 730-kA, 40-ns Hermes III gamma ray simulator.² In these electron beam accelerators, the currents from two or more pulse forming lines (PFLs) are added in high power linear induction cavities. The cavity outputs are then added in a self magnetically insulated transmission line (MITL)³. The MITL outer conductor is established by the cavity bores and has a constant diameter. The inner conductor is coaxial with the cavity bores and extends through the length of the cavities. It

DISCLAIMER

This report was prepared as an account of work sponsored by an agency of the United States Government. Neither the United States Government nor any agency thereof, nor any of their employees, makes any warranty, express or implied, or assumes any legal liability or responsibility for the accuracy, completeness, or usefulness of any information, apparatus, product, or process disclosed, or represents that its use would not infringe privately owned rights. Reference herein to any specific commercial product, process, or service by trade name, trademark, manufacturer, or otherwise does not necessarily constitute or imply its endorsement, recommendation, or favoring by the United States Government or any agency thereof. The views and opinions of authors expressed herein do not necessarily state or reflect those of the United States Government or any agency thereof.

MASTER

DISCLAIMER

This report was prepared as an account of work sponsored by an agency of the United States Government. Neither the United States Government nor any agency thereof, nor any of their employees, makes any warranty, express or implied, or assumes any legal liability or responsibility for the accuracy, completeness, or usefulness of any information, apparatus, product, or process disclosed, or represents that its use would not infringe privately owned rights. Reference herein to any specific commercial product, process, or service by trade name, trademark, manufacturer, or otherwise does not necessarily constitute or imply its endorsement, recommendation, or favoring by the United States Government or any agency thereof. The views and opinions of authors expressed herein do not necessarily state or reflect those of the United States Government or any agency thereof.

DISCLAIMER

Portions of this document may be illegible in electronic image products. Images are produced from the best available original document.

is reduced in diameter at the feed gap of each successive cavity to increase the MITL impedance. The impedance of each MITL section is set such that the current through each cavity is constant, and the voltage at any point through the system is derived by the sum of the preceding cavity voltages. Under normal operating conditions, the MITL is used with the inner conductor as the cathode stalk and it is terminated with an electron beam diode load. The overall system, from the PFLs to the diode, has been demonstrated to be between 87% and 100% efficient when operated in negative polarity.¹ Similar efficiencies have been demonstrated with the 16-TW, 20-stage Hermes-III accelerator.²

We are presently investigating the feasibility of applying this technology to an ion beam accelerator for the inertial confinement fusion (ICF) program. We have developed a conceptual design of a light ion beam driver for a Laboratory Microfusion Facility (LMF) that uses accelerator modules very similar to Hermes III.⁴ A key issue in these designs is the performance of the adder MITL when it is operated in reversed polarity with the inner conductor positive.

A reversed polarity experiment has been performed on Hermes III.⁵ Data from this test indicates efficient energy transport through the adder, but current flow within the MITL is significantly different than in the negative polarity.

HELI A has been reconfigured with the inner conductor of the adder as the positive electrode (anode), so that the voltage adder efficiency, component interaction, accelerator reliability, and MITL current flow in a positive polarity system can be further investigated. The polarity reversal was accomplished by removing the inner conductor of the MITL and installing it from the opposite end of the system. This in effect grounds the negative end of the cavity system instead of the positive end. The energy storage, pulse forming components, and cavities are operated in a negative polarity as before. For these experiments, the accelerator was operated with two different MITL impedance configurations, with and without extension sections, that provide up to 14 ns of round trip time isolation between the diode load and the adder section.

System Description

Figure 2 is a schematic drawing of the positive polarity adder system. The diode A-K gap is adjustable from a short circuit to approximately a 7-cm spacing. Table 1 lists the free space impedance at each cavity bore for the two MITL adder center conductors. These are the same conductors that were used in the negative polarity configuration. The free space impedance with conductor A was selected for "matched impedance" MITL operation in negative polarity. This was accomplished by making the operating impedance of the n^{th} MITL section approximately equal to nZ_o , where Z_o is the "source impedance" for each of the cavities. Conductor B was selected for "overmatched" operation.

Table 1. Free Space Impedance of the MITL Adders

Cavity #	Conductor A* Imped. in Ohms	Conductor B** Imped. in Ohms
1	7.2	10.1
2	12.4	17.6
3	17.2	24.8
4	22.0	31.9

MITL extension sections can be inserted between cavity #4 and the diode. In each case, these extension sections maintain the free space impedance established at cavity #4. Also shown in Fig. 2 are current monitor locations along the inner conductor of the MITL after each cavity gap feed. There are four monitors at each location, equally spaced on the circumference of the inner conductor. There are also current monitors located on the inner and outer conductors near the diode load. The MITL current monitors are made up of B-dot current loop pairs contained within a common housing. The loops are rotated 180° so that one output is negative polarity and the other positive. The two loop outputs are routed to a Balun unit, where one signal input is inverted and then both inputs added. This process cancels induced cable noise signals, while preserving the current signal. This common mode rejection scheme has proven effective in measuring currents flowing within the MITL. Single-loop B-dot monitors and V-dot monitors, that are located at each cavity vacuum insulator stack, provide a measurement of the input power to the MITL adder.

System Performance

Figure 3 is a sample of current waveshapes measured at positions A1 through A4 in the adder section of HELIA when operated in positive polarity (see Fig. 2). These photos show that current along the inner conductor is constant and that there is not any detectable current loss from the outer to inner conductor in the MITL adder section.

Figure 4 shows a sample of time correlated voltage and current waveforms. The voltage waveform is the algebraic sum of the voltages measured at each of the four cavity vacuum insulator stacks. The current pulse was total current measured by a B-dot monitor in the inner conductor of the adder section.

Figure 5 is a plot of several shots showing current flow along the cathode and anode within the system. Figure 5a is a plot of boundary current flowing in the adder section of the MITL as measured at positions IC1 through IC4, and boundary current downstream of the adder section at positions C5 (see Fig. 2). The difference between current measured at position IC4 and the total current flowing in the system is the sheath current within the adder section. Sheath current electrons are emitted from the surfaces of the cavity bores. The kinetic energy obtained by electrons in the sheath when they are accelerated to the anode is dependent upon the potential at which they are emitted. The data plotted were obtained with diode A-K gaps ranging from 2.8 cm to 6.8 cm. As can be seen, the measured boundary current decreases gradually in successive cavities. This decrease of about 10% to 15% of the total current is sheath electrons that are flowing within the adder section. Because the sheath electrons are not emitted at full potential, these electrons may be considered a loss current to an ion diode. Since these electrons would have an average energy corresponding to half of the full voltage potential, they would represent a power loss of less than 10%.

Figure 5a also shows a marked decrease in boundary current measured at position C5 downstream of cavity #4. This decrease becomes more significant with large diode A-K gaps. Boundary current is 30% of total current with a 6.8 cm A-K gap, compared to 78% of total current with a 2.8 cm A-K gap. Because of the proximity of the diode and its configuration, this decrease is more sensitive to diode A-K variations than in the case where an MITL extension is used.

Decreasing boundary current in the MITL just beyond the final cavity is more readily defined in the Hermes-III positive polarity experiment because of the transit time isolation between the adder section and the diode load. Sheath current electrons that are contributed after the last cavity are near cathode potential and do not necessarily represent a loss if those electrons can be retrapped and/or coupled to an ion diode.

Figure 5b is a plot of anode currents measured through the system along the inner conductor. For A-K gaps ≤ 3.8 cm, the current is approximately constant. With the 6.8 cm spacing, a reduced current is seen at positions A4 and A5. For the larger gaps, this may be an increased system loss or electrons may again be bypassing these monitor locations.

In the absence of loss between the 3rd and 4th cavity feeds gaps, the difference between currents measured at IC4 and C5 is sheath current due only to the electrons emitted downstream of the 4th feed gap. Figure 6 shows a comparison of these measured currents. Figure 7 shows a voltage calculation done for a shot in which the A-K gap was set at 3.8 cm. The voltage can be calculated from these currents in the same manner that is appropriate for a single-cathode MITL.⁶ This calculated peak voltage of approximately 2.7 MV agrees with peak voltage measured with filtered CR-39 nuclear tracking film.⁷ Figure 8 is a comparison of waveshapes recorded at position C5 and A4, boundary and anode currents respectively, for this shot.

Figure 9 is a comparison of the operating impedance between positive and negative polarity with the "overmatched" MITL. The data were taken without an MITL extension, but data acquired with a one meter extension indicates little difference, except that the curve shifts approximately 0.5 cm to the left. It has been shown that in negative polarity the ramped portion of the plots represent the load dominated region, and the plateau sections are established by the MITL operating impedance.⁸ The data presented here were calculated using the ratio of the algebraic sum of the four cavity voltages and total current, and is plotted as a function of A-K gap. Filtered CR-39 packs were also used to record peak voltage on several shots. Peak voltages recorded by the CR-39 agreed with summed voltages corrected for time coincidence with the total current pulse, when the A-K gap was ≥ 3.8 cm. When smaller gaps were

used, the summed voltage and CR-39 measured voltage no longer agreed, with the CR-39 voltage being substantially lower.

These plots indicate that the system is matched by a smaller load impedance in positive polarity as compared to negative polarity. Thus, at a given equilibrium voltage, the system operates with a higher total current in positive polarity because of increased electron flow. In the case of the "matched impedance" adder, a gap of approximately 3.8 cm provides a nearly matched load to the positive MITL adder. For the negative "matched impedance" adder, a gap of about 6 cm provides an equivalent match. The ratio of the positive to negative A-K gap is about 0.64. This ratio agrees with the ratio of the operating MITL impedance assuming minimum current, single-cathode, self limited MITL flow⁶ and a full gap MITL flow, where the electron sheath extends across the entire MITL gap.

Future Plans

Design and fabrication of hardware for an extraction ion diode experiment have been completed. This experiment is now being fielded on HELIA, with the aim of investigating issues of coupling energy to an ion diode, and to establish criteria for future diode studies.

A design has been completed, and hardware fabrication has begun, for the upgrade of HELIA from its present four cavity system to a ten cavity system named SABRE. SABRE-system output parameters will be 10 MV, 250 kA, at 40-ns FWHM. This new facility will make it possible to do a more in-depth study of a positive polarity system at higher voltage, and will provide another test bed for future ion-diode experiments at higher voltage. Various methods to maximize the power that can be coupled into an ion diode will be investigated.

Conclusions

The experiment has shown that HELIA can be 85-95% efficient in current transport through the positive polarity adder, and that overall system reliability is not adversely effected by the polarity reversal. The system behavior, as demonstrated by the data presented here, is shown to be

essentially the same in positive polarity as it is in negative polarity.

Due to the decrease in measured current flowing through each successive cavity, and given a constant total current, the sheath current after each cavity feed gap is increasing correspondingly. The decreasing current flow in the cavities translates to an increase of voltage within those cavities. This voltage increase is more significant in larger facilities, and can be seen clearly in the reversed polarity experiment done on Hermes III.

Positive polarity system experiments will continue on the new 10-MV SABRE facility. Emphasis will be on improved diode design, techniques of minimizing losses, and coupling energy to an ion beam diode.

Acknowledgements

The authors wish to express their gratitude to W. G. Adams for his efforts in running and maintaining the HELIA facility during these experiments, and for his contribution in gathering and analyzing the data.

References

1. J. J. Ramirez, et al., "The Four Stage HELIA Experiment," in Proceedings of the 5th IEEE Pulsed Power Conference, 1985, p. 143.
2. J. J. Ramirez, et al., "The Hermes-III Program," in Proceedings of the 6th IEEE Pulsed Power Conference, 1987, p. 294.
3. R. C. Pate, et al., "Self-Magnetically Insulated Transmission Line (MITL) System Design for the 20-Stage Hermes-III Accelerator," in Proceedings of the 6th IEEE Pulsed Power Conference, 1987, p. 478.
4. D. L. Johnson, et al., "A Conceptual Design For an LMF Accelerator Module," to be published. Particle Accelerator Conference, Chicago, IL, March 1989.

5. D. L. Johnson, et al., "Hermes-III Positive Polarity Experiment," in these proceedings.
6. C. W. Mendel, Jr., D. B. Seidel, and S. E. Rosenthal, Laser and Part. Beams 1, 311, 1983.
7. J. Bailey, et al., Bull. Am. Phys. Soc., 32, 1873, (1987).
8. T. W. L. Sanford, et al., "Impedance of an Annular-Cathode Indented-Anode Electron Diode Terminating a Coaxial MITL," J. App. Phys., 63, 681, (1988).

Figure Captions

Fig. 1 Photograph showing the HELIA facility.

Fig. 2 Schematic drawing of the positive polarity adder system.

Fig. 3. Current waveshapes measured along the inner conductor of the "over matched" positive polarity adder with a 3.8 cm A-K gap.

Fig 4. Time correlated comparison of the summed cavity voltage and the total current flowing in the system.

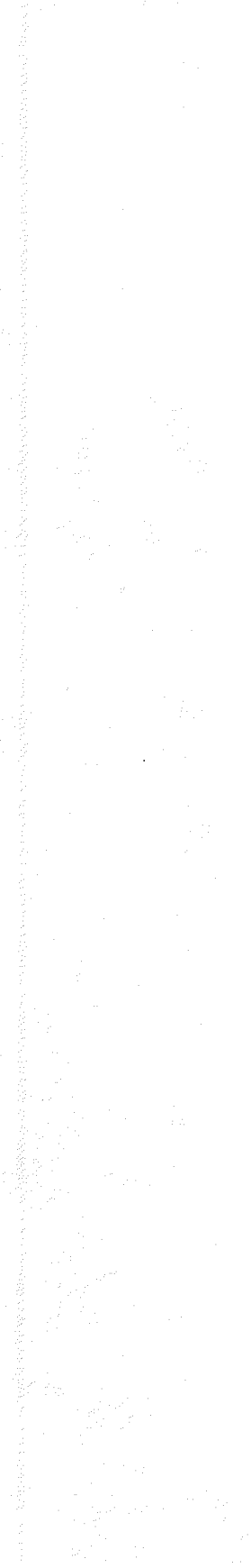
Fig. 5 Plot of measured currents with the "overmatched" adder in positive polarity, a) boundary current, b) anode current.

Fig. 6 Current waveforms measured at position IC4 and C5.

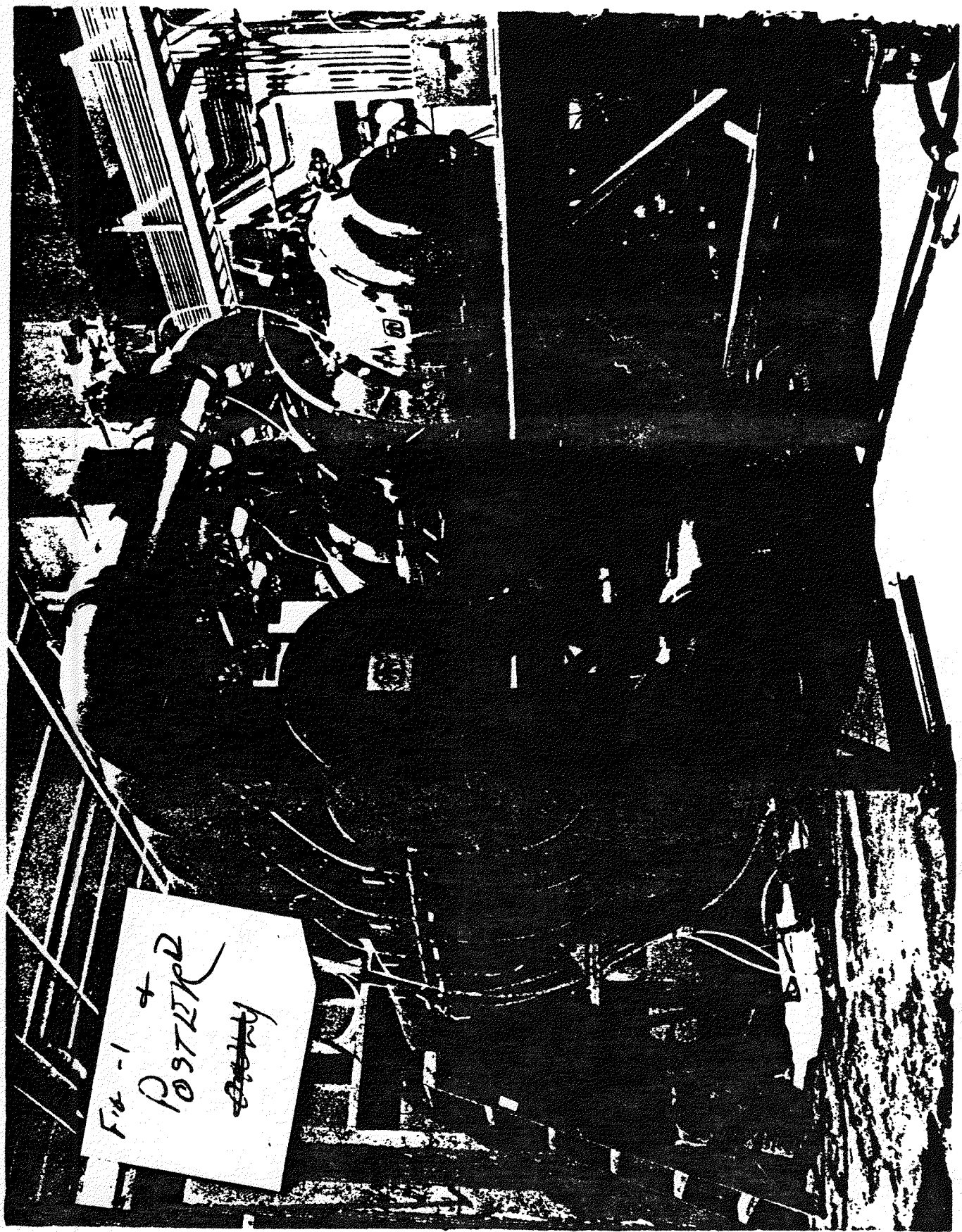
Fig. 7 Calculated voltage using IC4 and C5 current waveforms with the "overmatched" MITL and a 3.8 cm A-K gap.

Fig. 8 Comparison of boundary current and total current in positive polarity near the diode with a 3.8 cm gap.

Fig. 9 Comparison of positive and negative polarity operation using the "overmatched" MITL adder.



C84 - 7314



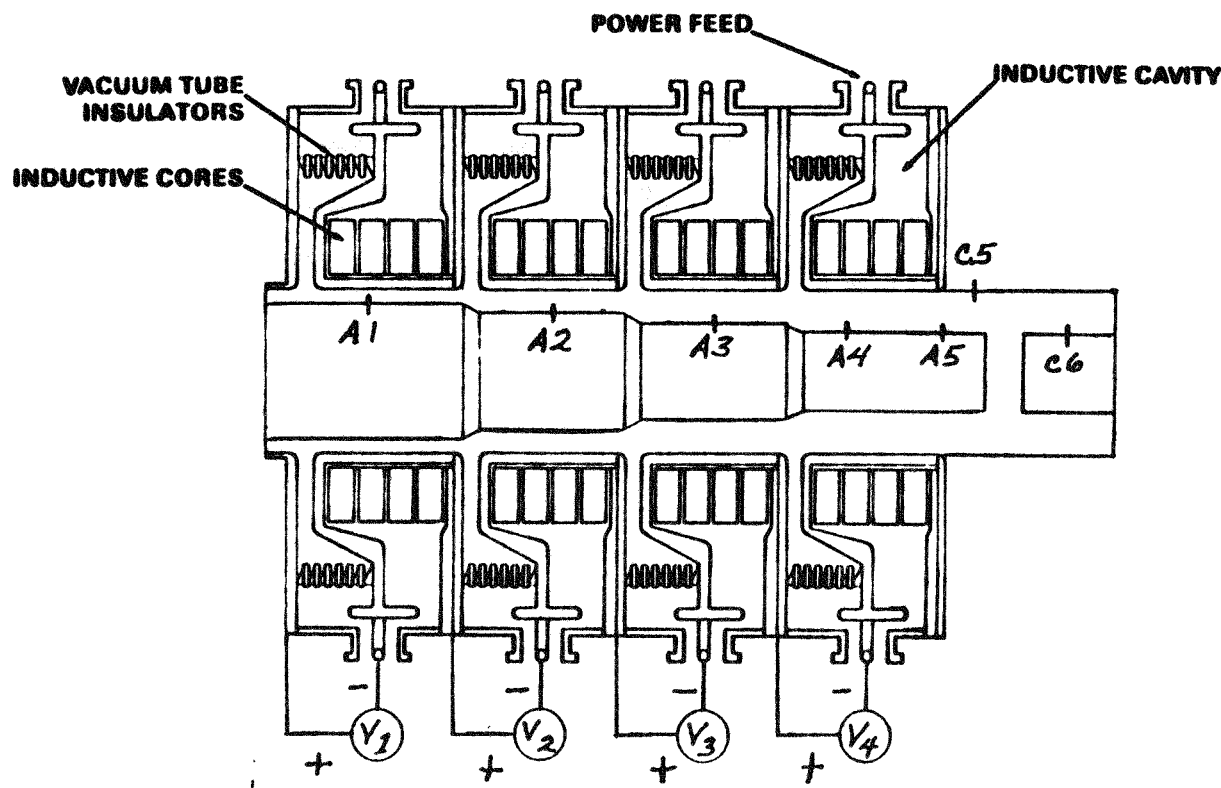


FIGURE 2. *Diagram of the 1000-watt
 ADAMK 3157A 110*
 2

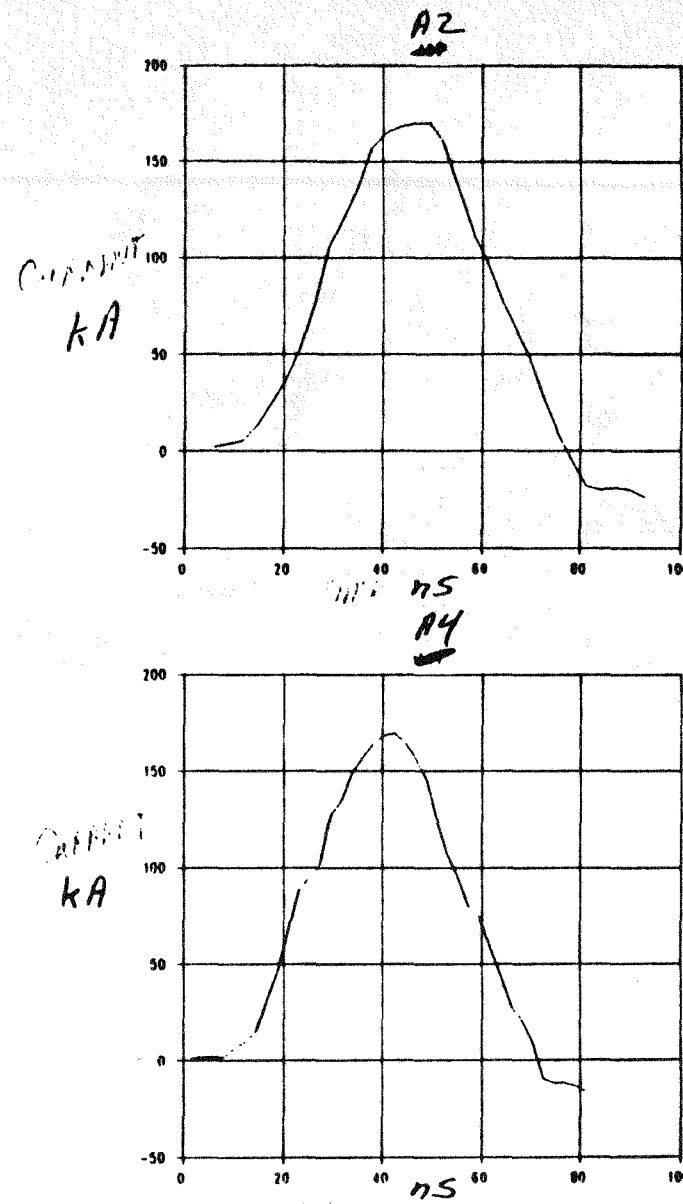
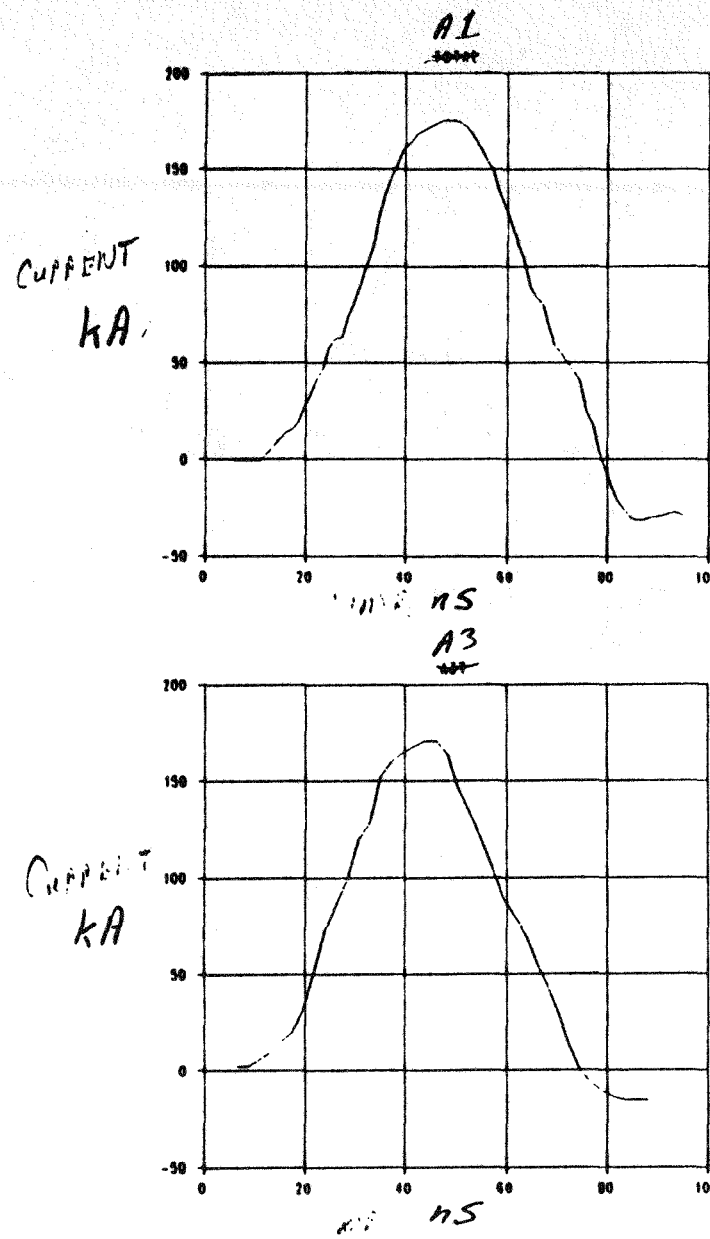
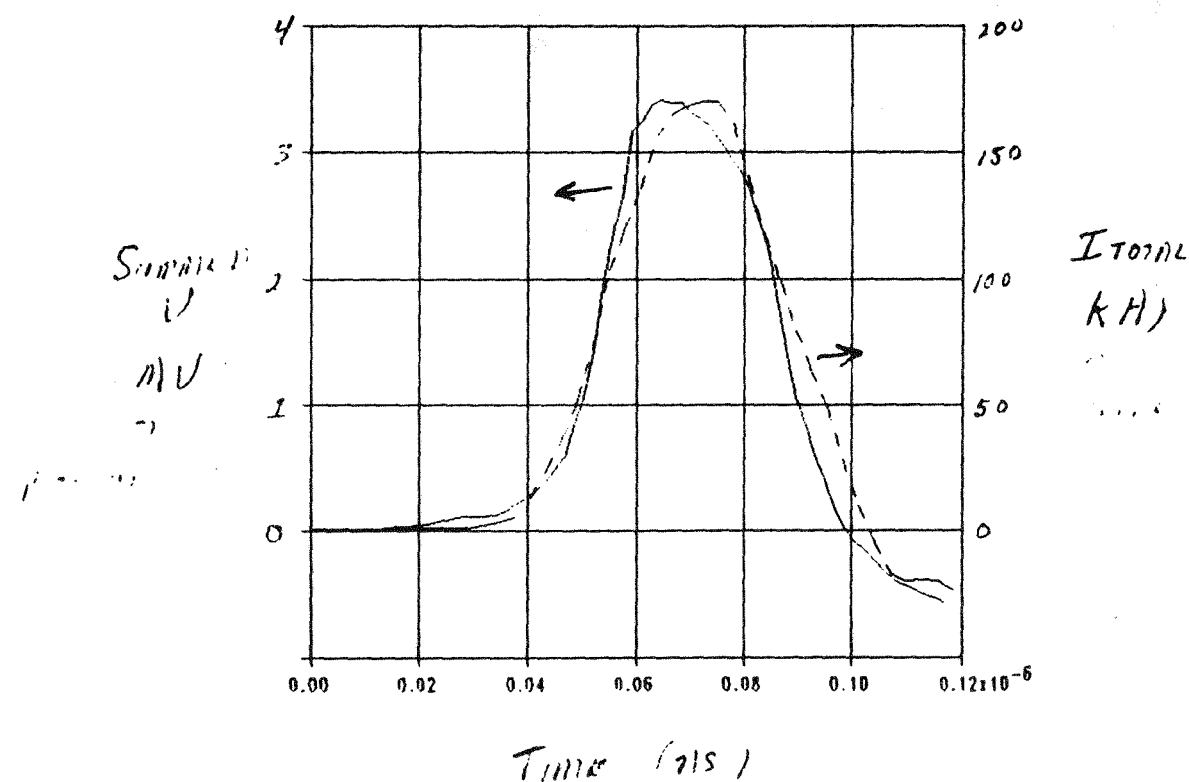
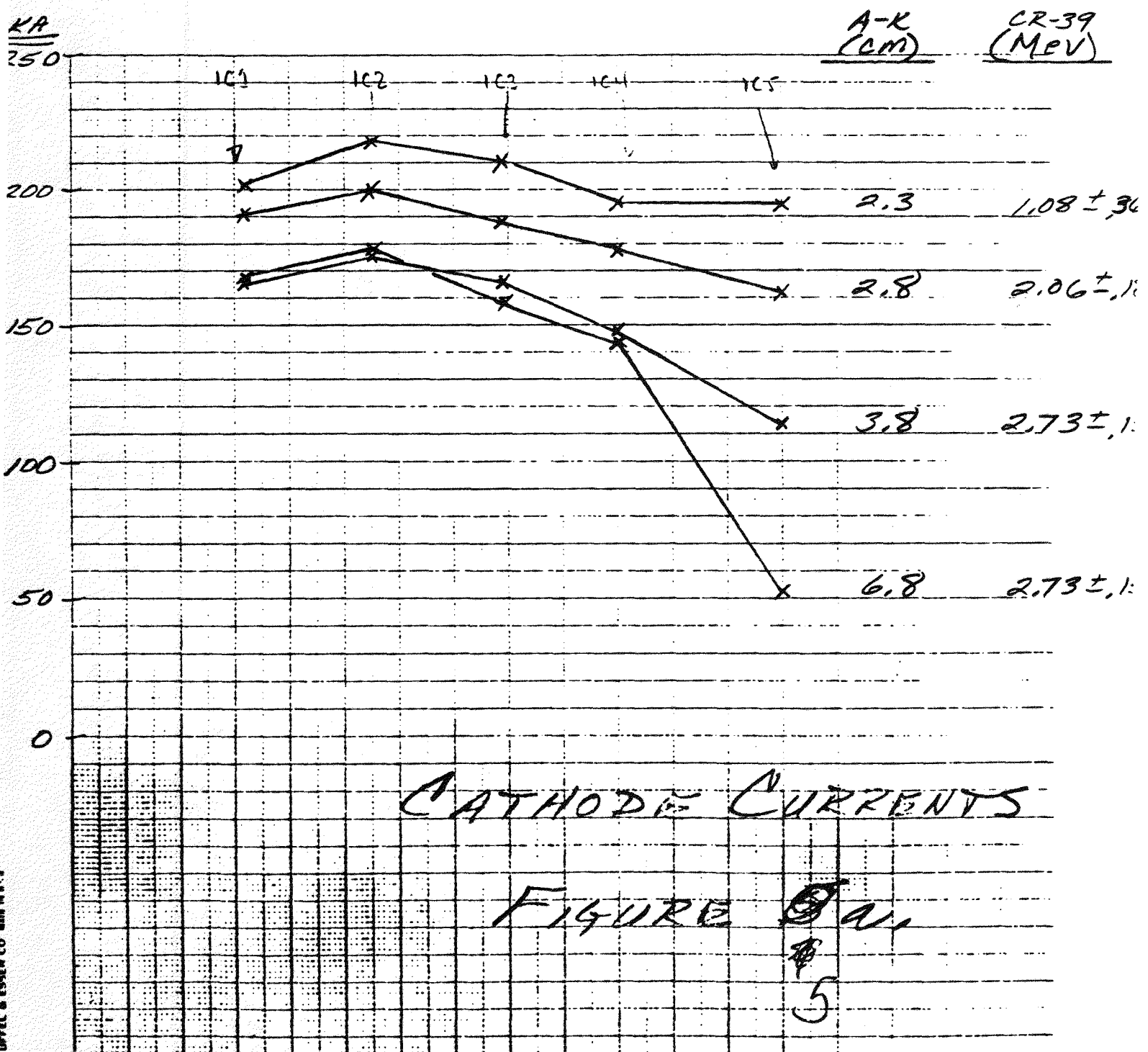
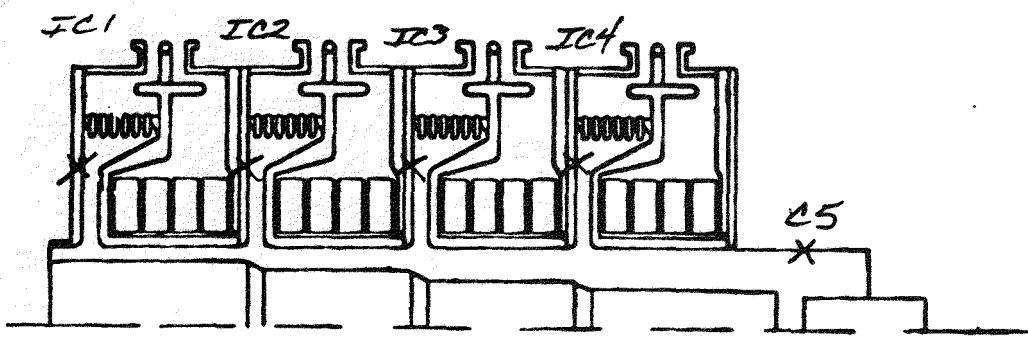
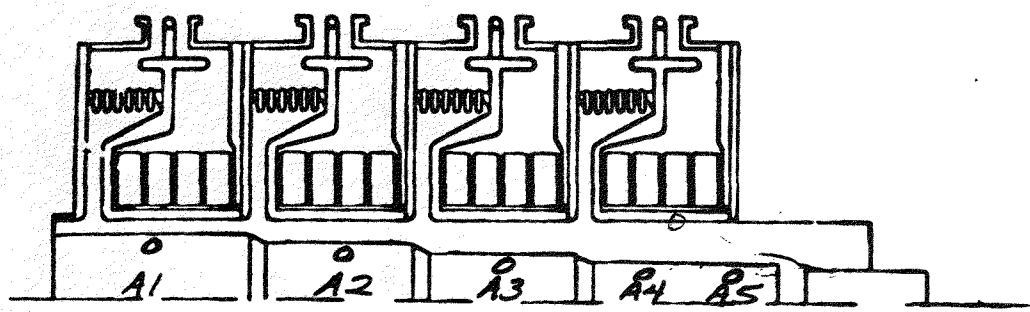


FIGURE 3. CURRENT WAVESHAPES ALONG THE INNER CONDUCTOR
OF ADDER B WITH A 3.8 cm A-K.

13 4



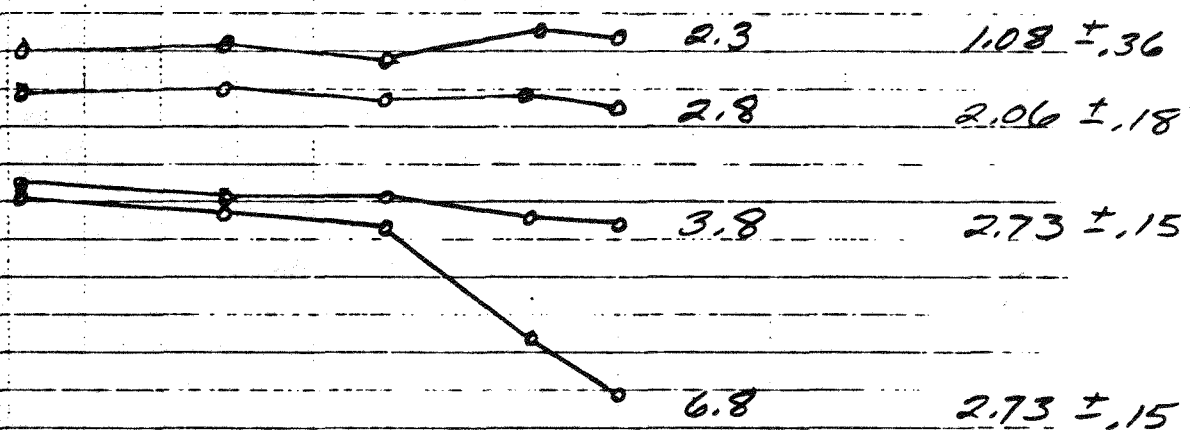




KA
250

A-K
(cm)

(CR-39
(MeV)



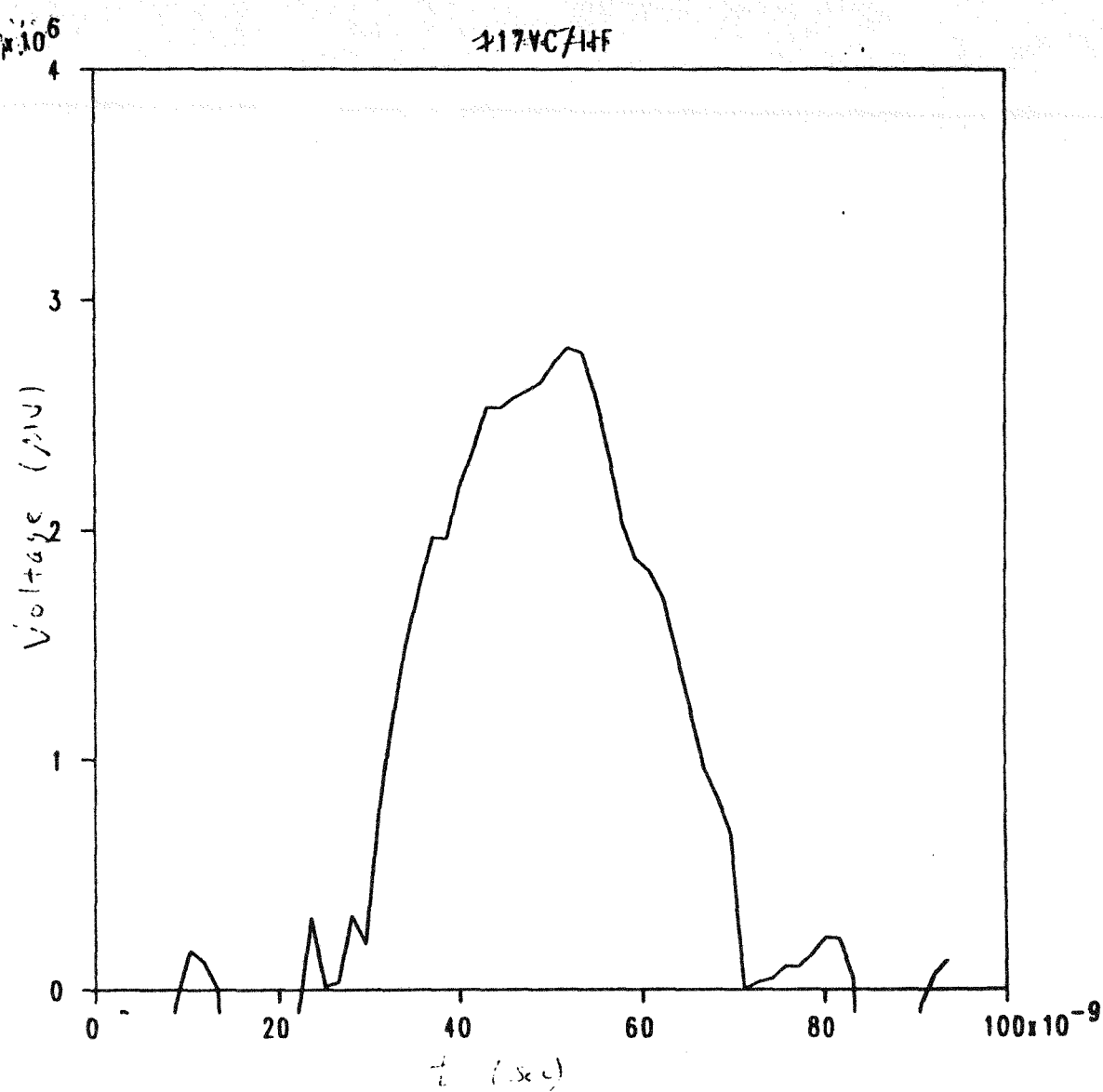
ANODE CURRENTS

FIGURE 5b

5

5/18/89 13:46:43

2174C44F



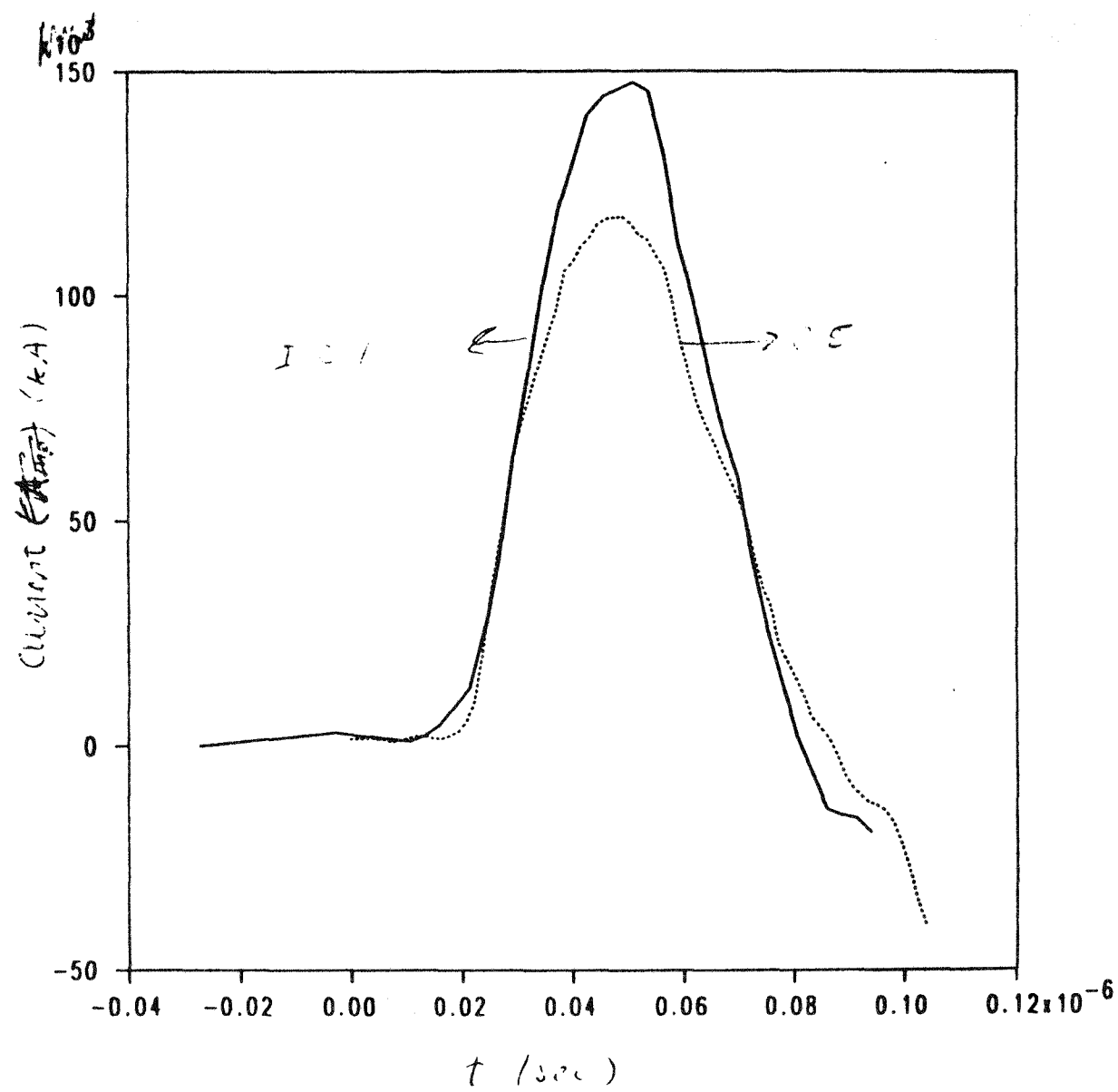
~~SEE: 8/89~~

2.75 mV

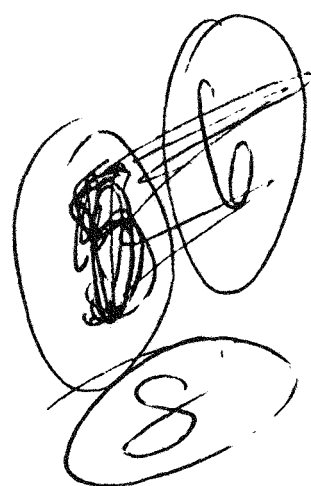
5/18/89 13:45:42

1 117CT3
2 117CT5

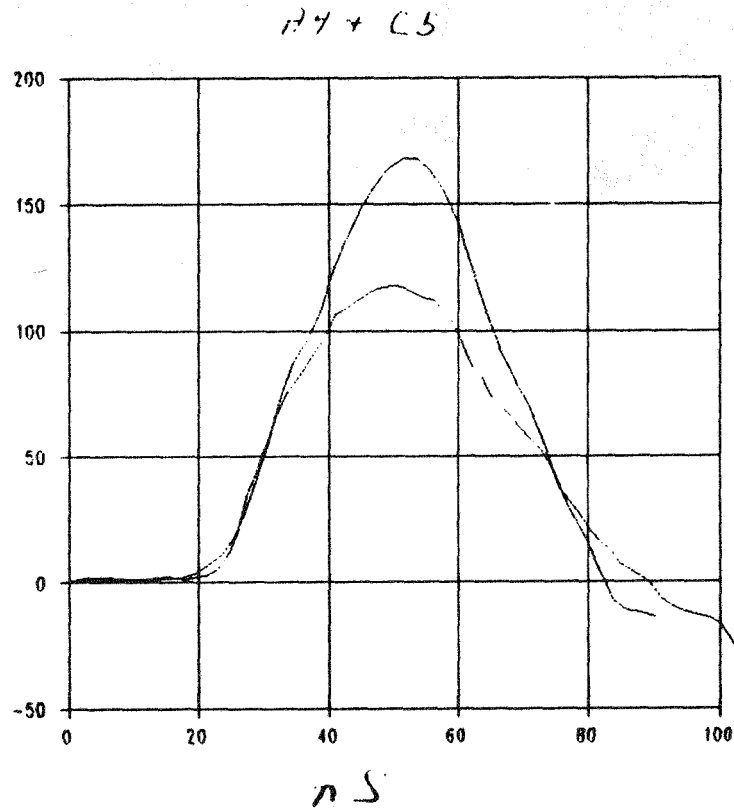
~~test~~
Fig 8
~~117CT3~~
~~117CT5~~



5/18/89



k/1



~~FIG. 3.~~ COMPARISON OF BOUNDARY CURRENT
AND TOTAL CURRENT NEAR THE DIODE.

~~2 NC / 1012U CURRENT~~

22

20

18

16

14

12

• NEGATIVE

× POSITIVE

1 2 3 4 5 6 7 8

DIODE A-K GAP

(cm)

9

FIGURE 2b. COMPARISON OF POSITIVE
AND NEGATIVE OPERATION USING ADDER B.